Supplementary Materials for

Calcium-Sensing Receptor Antagonists Abrogate Airways Hyperresponsiveness and Inflammation in Allergic Asthma

Polina L. Yarova, Alecia L. Stewart, Venkatachalem Sathish, Rodney D. Britt Jr., Michael A. Thompson, Alexander P.P. Lowe, Michelle Freeman, Bharathi Aravamudan, Hirohito Kita, Sarah C. Brennan, Martin Schepelmann, Thomas Davies, Zakky Cholisoh, Emma J. Kidd, William R. Ford, Kenneth J. Broadley, Katja Rietdorf, Wenhan Chang, Mohamed E. Bin Khayat, Donald T. Ward, Christopher J. Corrigan, Jeremy P.T. Ward, Paul J. Kemp, Christina M. Pabelick, YS Prakash* and Daniela Riccardi*

correspondence to: Riccardi@cf.ac.uk; Prakash.ys@mayo.edu

This PDF file includes:

Other Supplementary Materials for this manuscript include the following:

Materials and Methods

Western analysis of HEK293 cells: Stable expression of the human CaSR in HEK293 cells (CaSR-HEK) or of the empty vector, pcDNA3.1 (control, HEK-0) was carried out by as described elsewhere (*50*). Western analysis was carried out on 20 μg of protein lysates from CaSR-HEK or CaSR-0 out using standard SDS-PAGE with 10% gel and PVDF membrane, with β-actin (1:10,000, Abcam) as the loading control. Membranes were incubated overnight at 4 °C with a CaSR monoclonal antibody (ADD, 1:1000, Abcam) and detection of the primary antibody binding was carried out using a horseradish peroxidase-conjugated rabbit anti-mouse secondary antibody (1:10,000, Abcam).

Measurements of intracellular cAMP and IP_3 content: Cells from four non-asthmatic ("healthy") and three asthmatic patients (passage 2-4) were seeded into 60mm dishes at a density of 100,000 cells/plate and grown to confluence, after which they were exposed to 100 nM of the calcilytic NPS2143 for 15 minutes before proteins were harvested. cAMP and IP_3 measurements were carried out using ELISA kits from Alfa Aesar with the acetylated protocol and from MyBiosource, respectively, following the manufacturers' instructions.

FACS analysis: Airways were removed from WT and KO mice, the trachea and extralobular bronchi where carefully dissected under a microscope and the connective tissue removed. Airways were firstly incubated for 20 minutes at 37^{o}C in enzymatic PBS solution 1 (papain (1 mg/ml), dithiothreitol (DTT, 1 mg/ml), protease-free bovine serum albumin (BSA, 1 mg/ml)) and then for 10 minutes at 37^{o}C in enzymatic PBS solution 2. (collagenase (type XI, 2 mg/ml), soybean trypsin inhibitor (0.5 mg/ml) and 1 mg/ml BSA). The digested tissue was gently triturated and the supernatant containing the cells was resuspended in fresh PBS. Cells were fixed in 2% PFA for 15 minutes at room temperature and were then incubated with an anti-CaSR primary rabbit antibody (1:100, Anaspec) overnight at 4 ^{o}C. Cells were permeabilized using 0.1% Tween-20, 1% BSA in PBS for 1 hour and subsequently a goat anti-SM22α (1:250, Abcam) was applied for 1

hour at room temperature. The secondary antibodies (Alexa 488 conjugated goat anti-rabbit and Alexa 594 conjugated chicken anti-goat) were used at final dilutions of 1:400 in the permeabilization buffer containing 5% chicken serum for 1 hour. For the isotype controls, samples were incubated with the rabbit or goat IgG isotypes (Abcam) at the same dilutions as the primary antibodies. The samples were analyzed using a dual laser BD Canto flow cytometer (BD Biosciences) with DIVA software as per manufacturer's instructions. BD Comp-beads (BD Biosciences) were used to compensate for spectra spillover within the multicolor assay using unstained and single stained beads for each antibody. The unlabeled cells was used to set up baseline PMT so that <10% of the total events fell on the boundary of the FSC/SSC plot, and detectors were set with the population not exceeding the second log decade in each dot plot. Recorded data (~ 10,000 events) were further analyzed by FlowJo (single cell analysis software). Within the FSC/SSC gate, the debris was identified and only the live population was gated (P1). Doublets (cell clusters) were eliminated using FSC-A/FSC-H dot plot with the single cells identified along the diagonal of the plot and gated (P2). Gates P1 and P2 were combined for the next step of analysis creating gate P3. SM22α and CaSR were plotted against each other using the P3 population, where a quadrant gate was applied and the bottom left quadrant was positioned around the population of the isotype control.

Ca^{2+}_i imaging in mouse ASM: Mouse ASM cells, freshly isolated as described above, were seeded onto glass coverslips and allowed to adhere for 20 minutes at room temperature. The cells were subsequently loaded with fura-2 AM (4 μM) for 40 minutes. The solution was then changed to fresh buffer containing 0.5 mM Ca^{2+} for 30 minutes. Coverslips were placed into the chamber of an inverted microscope (Nikon IX71), and a rapid perfusion system (Intracel RSC160) was used to apply Ca^{2+}_o (1-5 mM), Gd^{3+} (0.1-1 mM), or ACh (3 μM). The images were recorded using an OptoFluor imaging system (version 7.8.2.0, Molecular Devices, LLC) or a Cairn monochromator-based fluorescence acquisition system.

CaSR expression in human eosinophils: Eosinophil cytospins from two healthy and three asthmatic subjects were fixed in ice-cold methanol. Cells were permeabilized with 0.1%

Tween-20 in PBS for 1 hour, after which samples were incubated with anti-CaSR primary rabbit (1:100, Anaspec) and with goat anti-human eosinophil peroxidase (EPX, 1:100, Santa Cruz) antibodies overnight at 4^{o}C. Negative controls were performed by omitting the primary antibodies. Secondary antibodies were goat anti-rabbit Alexa 488 and chcken anti-goat Alexa 594 (both at 1:400 dilution). Nuclei were stained with Hoechst (1:10000, 20 minutes). The cells were mounted using ProLong Gold mounting medium (Life Sciences). Images were acquired using an Olympus BX61 upright epifluorescence microscope using a 100x (oil) objective.

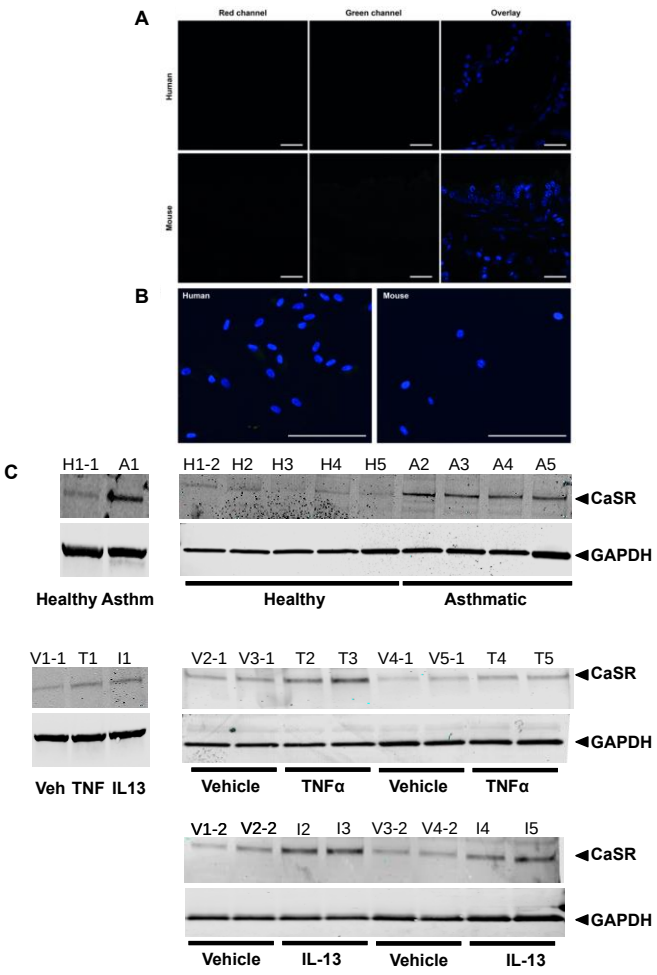

Fig. S1. Negative controls and original western blots for Fig. 1

(A) Negative controls (omission of the primary antibody) for the CaSR and SM22α immunofluorescence which are shown in Fig. 1A indicating the absence of CaSR (red channel) or SM22α (green) immunoreactivities in a human airway biopsy (top panel) or mouse intralobular bronchi (middle panel) (scale bar = 10 μm). (**B**) Human and mouse ASM cells showing absence of CaSR and aSM22α immunoreactivities when both primary antibodies were omitted (negative controls for Fig. 1B) (scale bar = 100 μm).

(C) Western blot replicates for Fig. 1D and E showing that there is increased CaSR protein expression in ASM of asthmatic patients compared to ASM of non-asthmatic ("healthy", upper panel), as well as in ASM of non-asthmatic which have been exposed to the pro-inflammatory cytokines TNF-α (20 ng/ml) or IL-13 (50 ng/ml) for 48hours, compared to vehicle controls (lower panels, N=5 for healthy and N=5 for asthmatic).

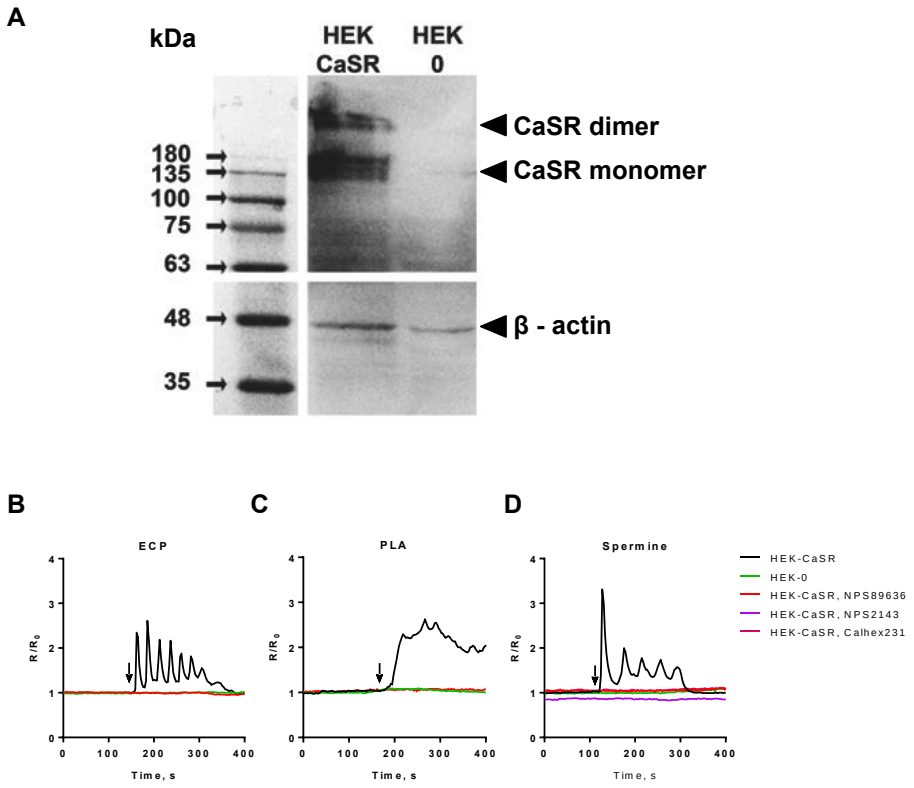

Fig. S2. Polycations increase $[Ca^{2+}]_i$ in by acting on the human CaSR

(**A**) Upper panel: Western blot showing CaSR immunoreactivity in cell lysate from HEK293 cells stably expressing (HEK-CaSR), but not in HEK293 cells stably transfected with an empty vector (control, HEK-0). Expected CaSR immunoreactivity is ~120-150 kDa (CaSR monomer) and 240-300 (CaSR dimer). Lower panel: Loading control western blot showing β – actin immunoreactivity in the same gel as above. Left: molecular weight marker (kDa: kilo Dalton).

(B-D) Representative individual traces of data summarized in Fig. 2A illustrating the changes in $[Ca^{2+}]_i$ induced by eosinophil cationic protein (ECP, 10 μg/ml) (**B**), poly-L-arginine (PLA, 300 μM) (**C**) and spermine (1 mM) (**D**). Polycations significantly increased $[Ca^{2+}]_i$ in HEK293 cells stably transfected with the human CaSR (HEK-CaSR), but evoked very little response in HEK293 cells stably transfected with an empty vector (control, HEK-0). The observed responses in HEK-CaSR were prevented by pre- and co-incubation with the calcilytics, NPS89636, NPS2143 or Calhex231, as indicated.

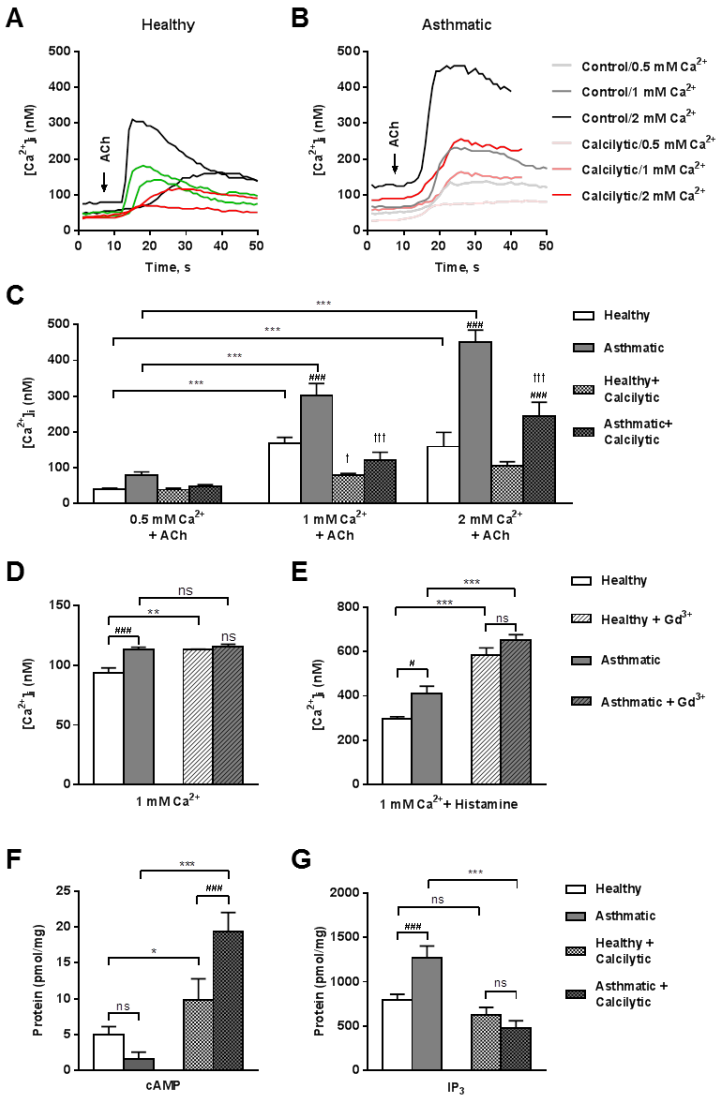

Fig. S3. Calcilytics prevent CaSR activation in human asthmatic ASM. Representative traces of changes in $[Ca^{2+}]_i$ in ASM cells from healthy patients (**A**) or asthmatics (**B**) showing response to ACh at different $[Ca^{2+}]_o$ (these $[Ca^{2+}]_o$ were changed 30 minutes prior to addition of agonist). Arrows indicate points of addition of the agonist, ACh. (**C**) The response to ACh (1 μM) was enhanced in the presence of $[Ca^{2+}]_o$ spanning the CaSR activation range. This effect was prevented by the calcilytic NPS2143. (**D**) Effect of Gd^{3+} on basal $[Ca^{2+}]_i$ in healthy and asthmatic ASM cells. (**E**) Effect of Gd^{3+} (0.1 mM) pre-treatment on responses to histamine (1 μM) in healthy and asthmatic ASM cells. (**F**) The calcilytic increased intracellular cAMP levels in the presence of 2 mM

$[Ca^{2+}]_o$ (when CaSR is likely to be maximally activated). This effect was particularly evident in ASM cells from asthmatics. (**G**) In ASM cells from asthmatics, baseline IP_3 levels were higher compared to ASM cells from non-asthmatic in the presence of 2 mM $[Ca^{2+}]_o$. The calcilytic reduced IP_3 levels, particularly in asthmatics. N=4-5 for healthy, and N=3-4 for asthmatic. Statistical significance was determined by two-way ANOVA, Bonferroni *post hoc* test (**C-G**), $^{***}P < 0.001$, significantly different from 0.5 mM (**C**), 1 mM (**D, E**), or 2 mM (**F, G**) $[Ca^{2+}]_o$ controls, $^{\#\#}P < 0.01$, $^{\#\#\#}P < 0.001$, statistically different from healthy within the same treatment group, $^{\dagger}P < 0.05$, $^{\dagger\dagger}P < 0.01$, $^{\dagger\dagger\dagger}P < 0.001$ statistically different from untreated within the same $[Ca^{2+}]_o$ group.

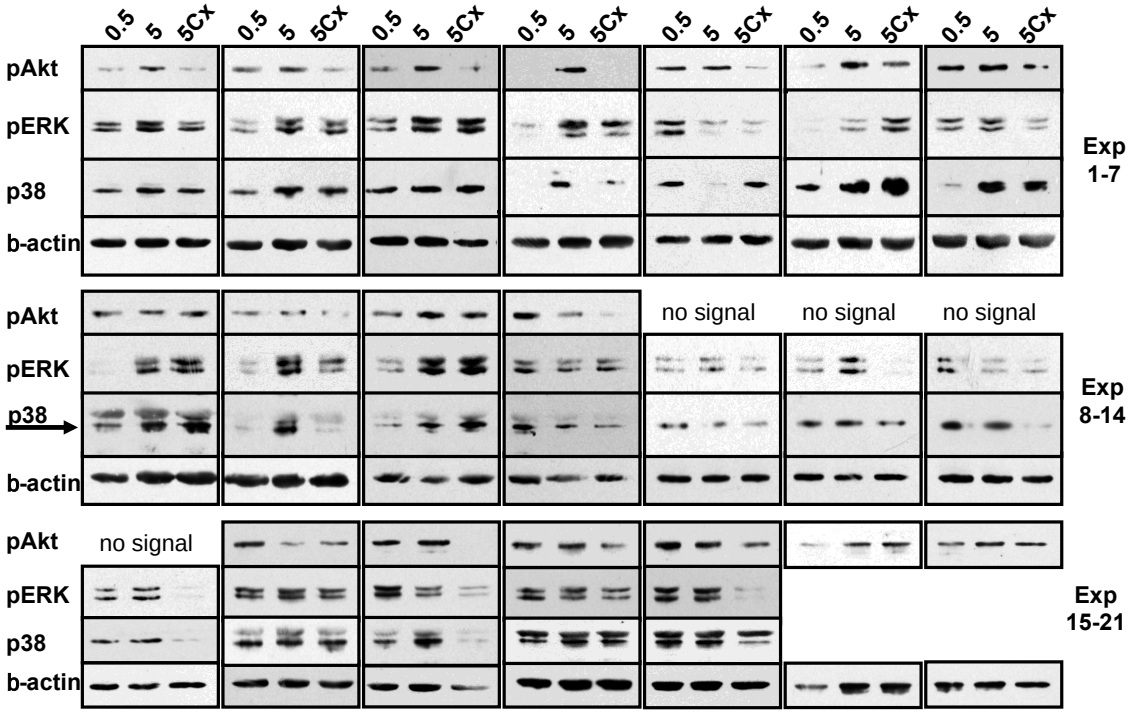

Fig. S4. Technical replicates of data presented in Fig. 2E and summarized in Fig. 2F. In human ASM cells, the calcilytic NPS2143 prevented phosphorylation of Akt, p38MAPK and ERK induced which could be induced by 5 mM Ca^{2+}_o. Cells were incubated for 5 minutes in experimental buffer containing either 0.5mM Ca^{2+} (0.5), 5mM Ca^{2+} (5) or 5mM Ca^{2+} plus 1mM NPS-2143 (5Cx) and then lysed in ice-cold RIPA-like buffer supplemented with protease and phosphatase inhibitors. The lysates were then processed for immunoblotting using antibodies against either phospho-Akt (Akt^{S473}), phospho-ERK (p44/42-$MAPK^{T202/Y204}$), phospho-p38 (p38-$MAPK^{T180/Y182}$), or β-actin (loading control). Immunoreactivity was quantified by densitometry, corrected for β-actin and statistical differences were determined by Friedman test (Dunn's post-test; GraphPad Prism, V6). No $pAkt^{S473}$ signal was detected for replicates 12-15 while for replicates 8-11, $p38^{MAPK}$ signal is indicated with an arrow, as the weak band above it results from incomplete stripping of the β-actin antibody. n=17-19 dishes from four independent experiments and using cells from two different non-asthmatic subjects.

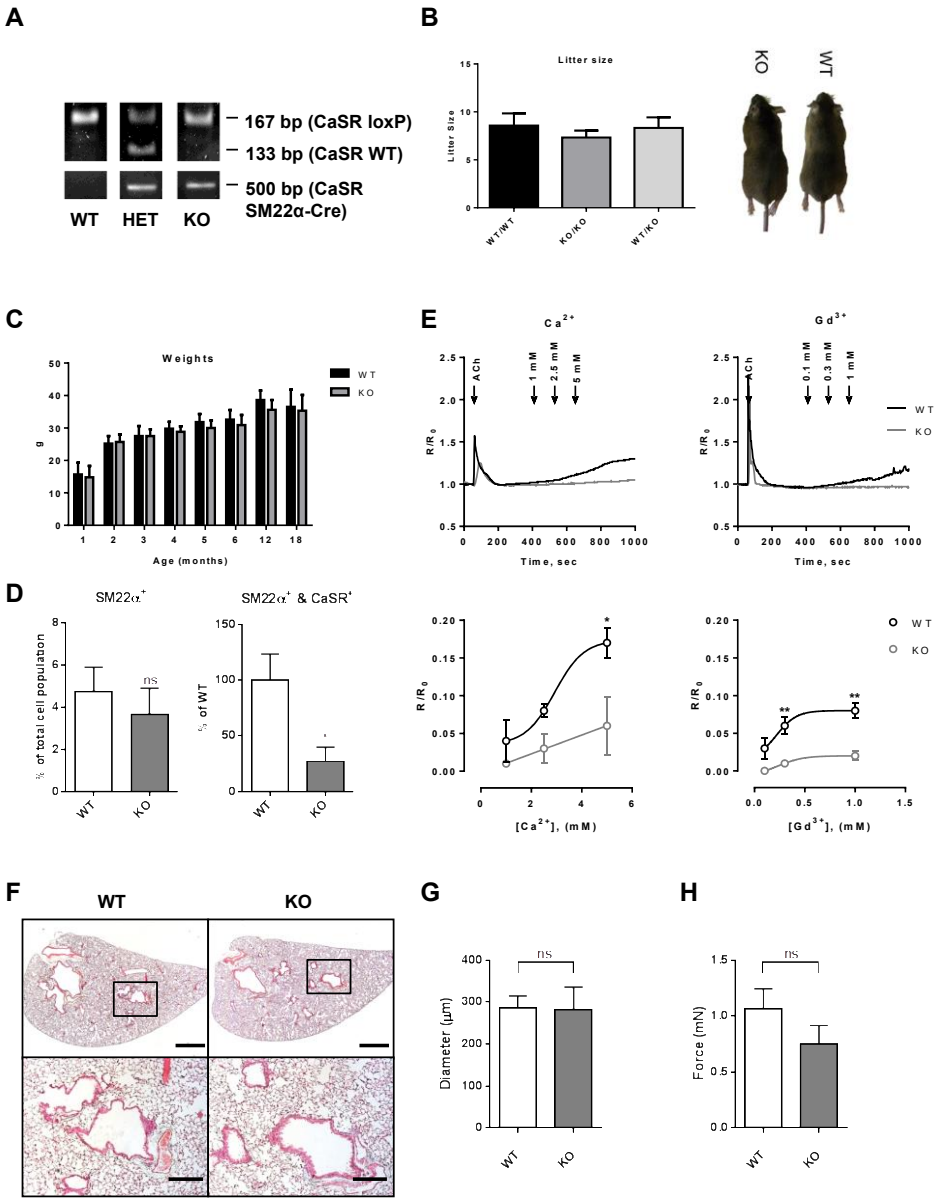

Fig. S5. Phenotypic characterization of the ^{SM22a}CaSR$^{\Delta flox/\Delta flox}$ mouse

(**A**) Molecular ablation of CaSR from ASM cells ($^{SM22a}CaSR^{\Delta flox/\Delta flox}$, KO) was confirmed by PCR. SM22α Cre-negative mice (WT) were used for these experiments; representative of > 50 animals genotyped for this study. Molecular CaSR ablation from ASM cells does not affect the appearance, litter size (**B**), body weight and survival rates (**C**) of KO mice compared to WT. Body weights of mice up to 18 month of age, mean ±

SD, N = 7-79 (WT) 7-46 (KO). (**D**) FACS analysis of SM22α-positive cells isolated from mouse airways showing that CaSR ablation from ASM cells does not affect the expression of SM22α in KO cells but results in a 75% reduction in CaSR immunoreactivity compared to that seen in WT. (**E**) Functional CaSR ablation from mouse ASM was confirmed by exposing cells isolated from WT and KO mouse intralobular bronchi to increasing concentrations of the CaSR agonists, Ca^{2+}_o (0.5-5 mM) and to the membrane-impermeant CaSR agonist, Gd^{3+} (100 μM-1mM). Single traces (upper panels) and dose-response curves (lower panels) showing that, in ACh-responding WT and KO ASM cells, Ca^{2+}_o induced an increase in $[Ca^{2+}]_i$ (fura-2 fluorescence), which was significantly greater in WT compared to KO ASM cells at 5 mM Ca^{2+}_o or ≥ 300 μM Gd^{3+} (WT, N = 3; KO, N = 3). (**F**) Lungs from KO mice appeared morphologically normal and comparable to those from WT animals (Masson trichrome staining; upper panel scale bars = 1 mm, lower panel scale bars = 0.25 mm). (**G**) The internal diameters of WT (N = 10) and KO (N = 8) intralobular bronchi were comparable. (**H**) In WT and KO intralobular bronchi, exposure to 40 mM KCl produced comparable contractions (WT, N = 14; KO, N = 12). For (**E**) statistical significance was determined by two way ANOVA with Bonferroni *post hoc* test, for (**G**) and (**H**), statistical significance was determined by two-tailed, unpaired Student's t-test, $*P < 0.05$, $**P < 0.01$, statistically different from WT.

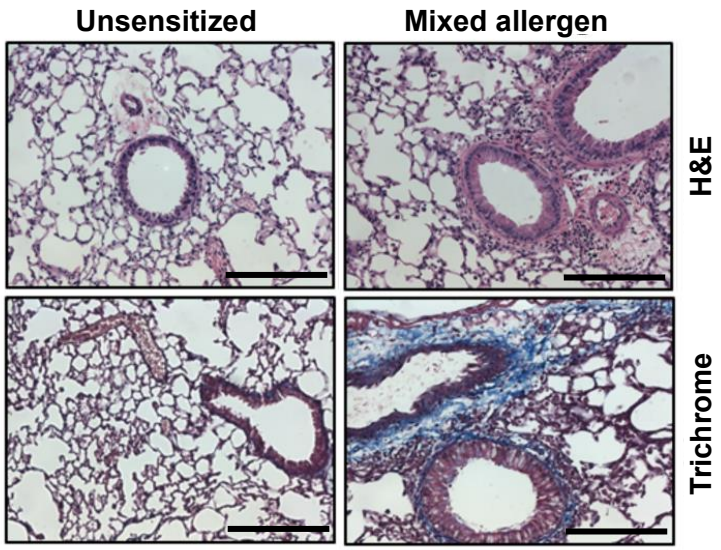

Fig. S6. Validation of the mixed allergen asthma model. Remodeling and inflammation, visualized by haematoxylin and eosin (H&E) and Masson-trichrome staining, are clearly visible in lungs from mixed allergen-sensitized mice (N = 3 mice per group). Scale bar = 400 µm.

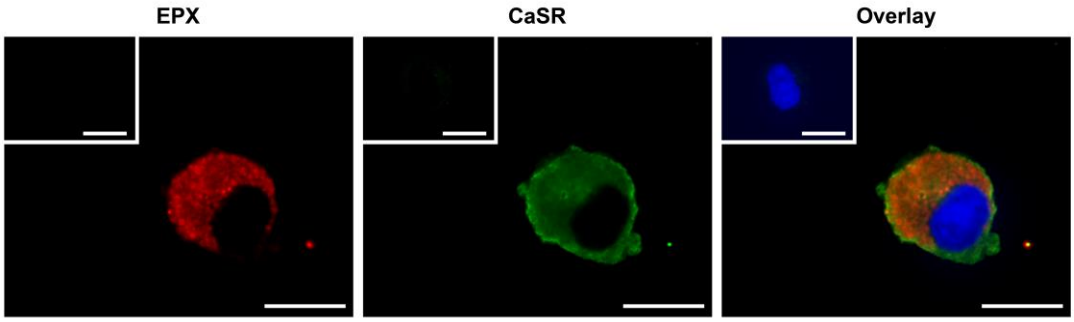

Fig. S7. CaSR expression in human eosinophils. CaSR immunofluorescence staining (green, middle panel) in a human eosinophil, identified by the marker, EPX (red, left panel). Overlay with nuclear counterstain Hoechst (right panel) and negative control staining (inserts, omission of primary antibodies) are shown. Scale bar = 10 μm.